Evanescent Wave Coupling in Hybrid III-V/SOI Nanolaser

A. Bazin[1], Y. Halioua[1,2], T. Karle[1], P. Monnier[1], G. Roelkens[2], I. Sagnes[1], R. Raj[1], F. Raineri[1,3]

[1]*Laboratoire de Photonique et de Nanostructures, CNRS-UPR20, Route de Nozay, 91460 Marcoussis, France*

[2]*Photonics Research Group, Department of Information Technology, Ghent University, B-9000 Ghent, Belgium*

[3]*Université Paris Denis Diderot, 75205 Paris, France*

ABSTRACT

Heterogeneous integration of III-V semiconductor compounds on SOI is one of the key technologies for next generation on chip optical interconnects. The use of photonic crystals nanolasers, within this context, represents a disruptive solution in terms of footprint, activation energy and ultrafast response. In this work, we study the evanescent wave coupling occurring between the nanolasers and a subjacent Si wire and demonstrate that more than 90% of the light is funneled into the Si circuitry.

1. INTRODUCTION

Heterogeneous integration of III-V semiconductor compounds on Silicon on insulator (SOI) is believed to be one of the key technologies for next generation on chip optical interconnects. Indeed, this hybrid platform combines the best of both material systems: on one hand, the CMOS compatibility and the predispositions of silicon to be used for fabricating an ultra compact low loss optical circuitry; on the other hand, the versatility of III-V semiconductors for making laser sources and active devices. This approach was recently used for demonstrating laser emission [1,2]. In this article, the concept of hybrid Si/III-V semiconductor photonics is scaled down to nanophotonics. III-V Photonic crystal nanolasers are integrated with and coupled to SOI waveguides circuitry. This disruptive approach allows us to obtain low threshold hybrid lasers in the telecom window within a footprint as small as 5μm². We experimentally study the evanescent wave coupling in the device as a function of the structure parameters and show that more than 90% of the emitted light is funneled into the SOI wires.

2. DESIGN AND FABRICATION OF THE HYBRID STRUCTURE

The hybrid structure under study is schematically represented on Fig. 1a. It is a 2 optical level structure where one level is constituted by a single mode SOI wire waveguide and the other, by an InP-based photonic crystal nanocavity with 4 InGaAsP/InGaAs quantum wells embedded which emit at 1.55 μm. The 2 levels are separated by a low index layer which preserves the vertical optical confinement within the SOI waveguide and the PhC cavity. Coupling is ensured by the penetration the evanescent tail of the optical modes into the other level [3].

The chosen nanocavity is a "wire" cavity, which is a Fabry-Perot type cavity formed in a single mode wire waveguide (550 nm width and 255 nm height). High reflectivity mirrors are constituted by a single row of holes drilled into the material. The holes diameter and the pitch of the 1D lattice are fixed to be respectively at 177.5 nm and 370 nm to obtain a large high reflectivity bandwidth around 1.55 μm. The sizes of the 3 holes on each side of the cavity are tapered down in order to increase the quality factor by adapting the propagating guided mode to the evanescent mirror mode [4].

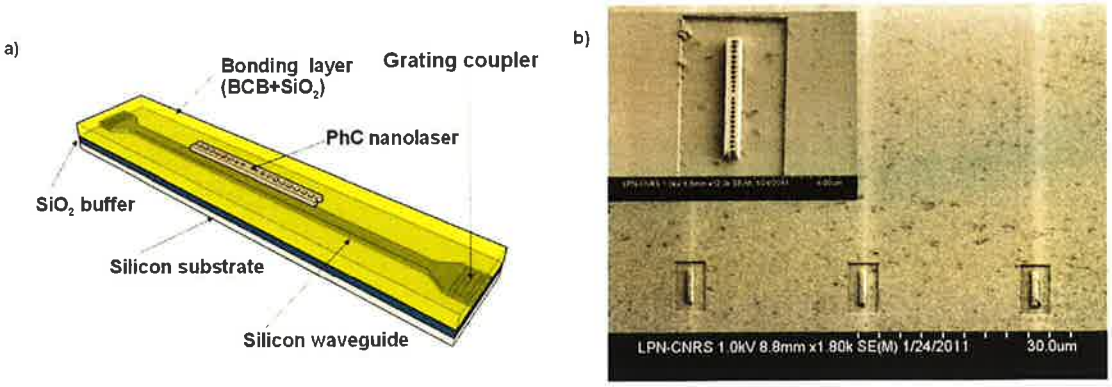

Figure 1. Hybrid III-V Semiconductor Photonic Crystal on SOI waveguide circuitry. a) Schematic view of the structure. b) SEM images of the fabricated sample. Inset: SEM image close-up of a wire cavity.

The fabrication of the hybrid structures is based on die-to-die adhesive wafer bonding and mix-and-match deep UV/electron beam lithography. The low index layer is a bilayer composed of a thin layer of BCB (80 nm) and a layer of SiO_2. 3 samples are fabricated with different SiO_2 thicknesses (200 nm, 300 nm and 400 nm).

978-1-4577-0882-4/11/$26.00 ©2011 IEEE

A scanning electron microscope picture of one of the fabricated structures is given on Fig. 1b where a wire cavity can be seen positioned on top of a SOI waveguide. The lithographic positioning has a demonstrated precision better than 30nm, which allows us to neglect the impact of the lateral offset between the two levels on the evanescent wave coupling [5].

3. LASER OPERATION

Laser emission is explored at room temperature by optically surface pumping the wire cavities using a modulated 800 nm laser diode The emitted light is collected via the gratings at the extremities of the 8 mm long SOI waveguides with SMF-28 optical fibres tilted at an angle of 10° to the surface normal and is analysed using a spectrometer equipped with a cooled InGaAs detector array. We plot in Fig. 2a, in log-log scale, the output peak power of the emitted light as a function of the absorbed pump peak power for a 450 nm-long cavity coupled to a 500 nm wide SOI waveguide (SiO_2 thickness is 400 nm). As expected for laser emission, the curve is S-shaped, with a threshold of 17 μW (external peak power 2 mW). The emission wavelength can be easily tuned by adjusting, for example, the cavity length as shown in Fig. 2b [6].

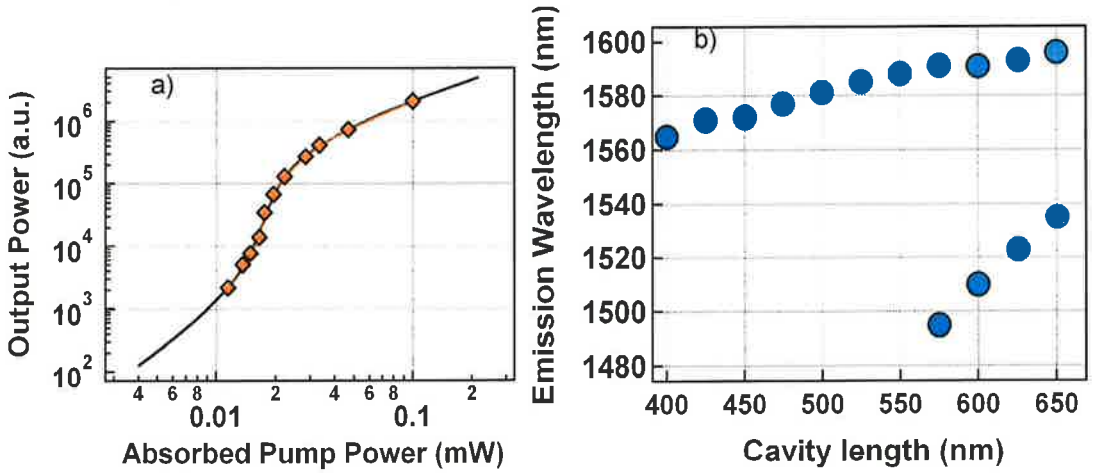

Figure 2: a) Intensity of the emitted light outputting the SOI waveguide as a function the absorbed pump power. The black line is a fit of the experimental data using the rate equations. b) Emission wavelength as a function of the cavity length, i.e. centre to centre distance between the first 2 tapered holes.

4. COUPLING EFFICIENCY

In order to determine the coupling efficiency of the laser emission into the SOI wire, we perform pump and probe measurements to obtain transmission spectra around the cavity resonant wavelength as a function of the pump power, i.e. as a function of the material gain or absorption.

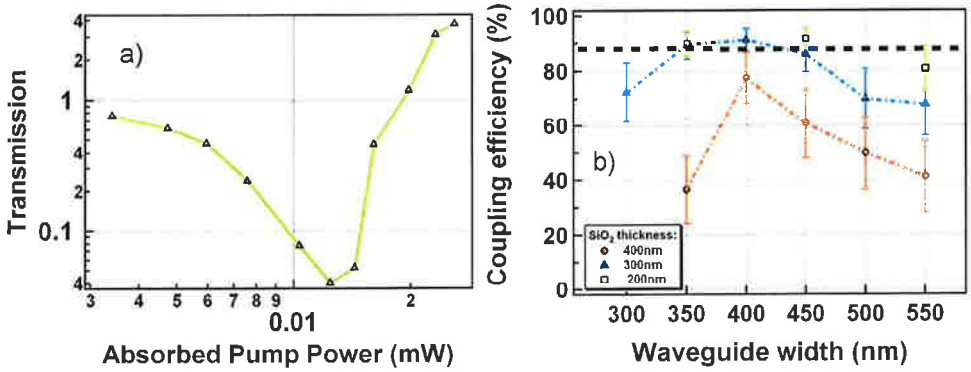

Figure 3: a) Transmission at resonance as a function of the pump power. b) Coupling efficiency of the emitted light into the SOI wire as a function of the structure parameters

As can be seen on Fig. 3a, the transmission at resonance firstly decreases when the pump power is increased reaching a minimum at 12.4 μW. By analysing the system with coupled-mode theory [3], we can show that, at this minimum, gain compensates exactly the unloaded cavity losses Γ_0 (cavity without waveguide).

The coupling constant to the SOI waveguide Γ_c can then be determined by measuring the full width at half maximum of the resonance in the transmission spectrum. Then, as the pump power is further increased, net gain is observed. In order to retrieve the coupling efficiency, which can be written

$$\eta = \frac{\Gamma_c}{\Gamma_0} \Big/ \left(\frac{\Gamma_c}{\Gamma_0} + 1 \right),$$

where Γ_0 is obtained by fitting the light-light curve with regular rate equations model for QWs laser. We performed this study for different types of samples where the thickness of the low-index layer and the width of the Si waveguides are varied in order to vary the strength of the evanescent coupling. The coupling efficiency can be controlled by adjusting the parameters of the structure and can reach values as high as 90% as seen on Fig. 3b. A good balance between Γ_c and Γ_0 has to be found in order to obtain large coupling as well as efficient laser emission.

ACKNOWLEDGEMENTS

The authors acknowledge for funding FP7 HISTORIC European Project and ANR Jeunes chercheurs French National project PROWOC. They also acknowledge COST MP0702 for collaborative work. The SOI wafers were fabricated within the ePIXfab European silicon platform. We thank Remy Braive for his help in the etching of photonic crystals and Bjorn Maes for useful discussion.

REFERENCES

[1] A. W. Fang et al., *Opt. Express* **14**, 9203-9210 (2006).
[2] J. Van Campenhout et al., *Opt. Express* **15**, 6744-6749 (2007).
[3] H. A. Haus, *Waves and Fields in Optoelectronics*, Englewood Cliffs, NJ. Prentice-Hall (1984).
[4] P. Velha et al., *New J. Phys.* **8**, 204 (2006).
[5] T. J. Karle et al., *J. Appl. Phys.* **107**, 063103 (2010).
[6] Y. Halioua et al., *J. Opt. Soc. Am. B*, **27**, 10 (2010).

IEEE Xplore DIGITAL LIBRARY

IEEE

Evanescent wave coupling in hybrid III-V/SOI nanolaser

Bazin, A. Halioua, Y. Karle, T. Monnier, P. Roelkens, G. Sagnes, I. Raj, R. Raineri, F.
Laboratoire de Photonique et de Nanostructures, CNRS-UPR20, Route de Nozay, 91460 Marcoussis, France

This paper appears in: Transparent Optical Networks (ICTON), 2011 13th International Conference on
Issue Date: 26-30 June 2011
On page(s): 1 - 3
Location: Stockholm, Sweden
ISSN: 2161-2056
E-ISBN: 978-1-4577-0880-0
Print ISBN: 978-1-4577-0881-7
Digital Object Identifier: 10.1109/ICTON.2011.5971135
Date of Current Version: 01 August 2011

ABSTRACT

Heterogeneous integration of III-V semiconductor compounds on SOI is one of the key technologies for next generation on chip optical interconnects. The use of photonic crystals nanolasers, within this context, represents a disruptive solution in terms of footprint, activation energy and ultrafast response. In this work, we study the evanescent wave coupling occurring between the nanolasers and a subjacent Si wire and demonstrate that more than 90% of the light is funneled into the Si circuitry.

1 We.P.1 A microfluidic platform integrated with tapered optical fiber for studying resonant properties of compact high index microspheres
*O.V. Svitelskiy, Y. Li, M. Sumetsky, D. Carnegie, E. Rafailov, **V.N. Astratov***

2 We.P.2 Chains of variable size spheres for focusing of multimodal beams in photonics applications
*A. Darafsheh, **V.N. Astratov***

3 We.P.3 Transient effects in high-Q whispering gallery mode resonators: Modelling and applications
*S. Trebaol, A. Rasoloniaina, **Y. Dumeige**, P. Féron*

4 We.P.4 Mode interaction in a circular shell ultrasonic cavity
***H. Kwak**, Y. Shin, J. Yang, S. Moon, S-Y. Lee, K. An*

5 We.P.5 On-chip mode-control in active silicon-based photonic molecule by complete photon confinement
***B. Qian**, K. Chen, S. Chen, W. Li, X. Zhang, J. Xu, X. Huang, C. Jiang*

6 We.P.6 Hybrid organic-inorganic nanostructures for integration with photonic atoms
***D. Savateeva**, D. Melnikau, Y.P. Rakovich*

7 We.P.7 Reconstruction of tunnelling emission pattern by using Husimi function
***Y. Shin**, S. Moon, H. Kwak, J. Yang, K. An*

8 We.P.8 Plasmon resonances in linear array of coupled silver nanowires
***N. Stogniy**, N. Sakhnenko, A. Nerukh*

9 We.P.9 Some features of plasmonic eigenmode nanolocalization in inhomogeneous metal-dielectric-metal slot waveguides
*D.A. Smirnova, **A.A. Zharov**, A.I. Smirnov*

10 We.P.10 Peculiarities of the interferences processes and their influence on the transmission spectrum of the ferrite-dielectric periodic structure bounded with the semiconductor layer
***O. Kostylyova**, A. Bulgakov*

11 We.P.11 Numerical analysis of transmission through a sub-wavelength metallic aperture or grating at visible and terahertz wavelengths
***M. Stolarek**, A. Pastuszczak, R. Kotyński*

12 We.P.12 Structural and nonlinear-optical properties of sprayed deposited Zr-Li codoped ZnO thin films
***K. Bahedi**, M. Addou, Z. Sofiani, M.A. Lamrani, A.R. Dounia, H. El Ouazzani, B. Sahraoui*

13 We.P.13 Third order nonlinear optical properties of novel tetrathiafulvalene-phenanthroline based dyads
***H. El Ouazzani**, K. Iliopoulos, V. Figà, P. Hudhomme, B. Sahraoui*

14 We.P.14 Photoluminescence of MgO thin films on Si (111) substrate, prepared by sol-gel method
***K. Bartkiewicz**, Z. Łukasiak, A. Zawadzka, P. P³óciennik, A. Korcala*

15 We.P.15 The effects of sprayed lithium and erbium codoped ZnO thin films on the structural and cathodoluminescent properties
***S. Bayoud**, M. Addou, M. El Jouad, A. El Hichou, J.C. Bernède, J. Ebothé*

16 We.P.16 Dye-interleaved nanocomposite: Indigo carmine and methyl orange in the lamella of zinc-aluminium-layered double hydroxide
***L. El Gaini**, M. Lakraimi, M. Bakasse*

17 We.P.17 Electric dipole moment and static first hyperpolarizability values of 4-(2-pyridylazo)resorcinol: High accuracy density functional theory computations
***A. Karaka°**, E. Ayhan*

18 We.P.18 The effect of thickness and doping on the nonlinear absorption behaviour of IIIA-VIA group amorphous semiconductor thin films
***U. Kürüm**, H.G. Yaglioglu, M. Yüksek, A. Elmali, A. Ate°, M. Karabulut, G.M. Mamedov, N. Gasanly*

19 We.P.19 Photoluminescence of electrochemically etched porous silicon coated with small-molecule based thin organic films
***Z. Łukasiak**, A. Zawadzka, P. P³óciennik, A. Korcala, K. Bartkiewicz*

20 We.P.20 Computer simulation of an operation of the 1.3-μm phosphide-based MQW TJ-VCSELs: Excitation of various transverse LP_{ij} modes
Ł. Piskorski

21 We.P.21 ZnO thin films doped with erbium: Elaboration, characterization and nonlinear optical properties measurements
*M. Addou, **Z. Sofiani**, K. Bahedi, H. El Ouazzani, V. Figà, B. Sahraoui*

22 We.P.22 Photoinduced transmittance at 1250 nm of InAs/InGaAs quantum dot based semiconductor optical amplifier measured via waveguiding configuration
*E. Jelmakas, **R. Tomašiūnas**, M. Vengris, E. Rafailov, I. Krestnikov*

23 We.P.23 Formation of the spontaneous surface relief grating under pulsed exposure
***S. Ahmadi-Kandjani**, L. Mazaheri*

24 We.P.24 Ghost imaging with pseudo-thermal light
***S. Ahmadi-Kandjani**, R. Kheradmand, N. Dadashzadeh*

25 We.P.25 Study of photoadmittance and admittance of porous silicon layers
A. Korcala, Z. Łukasiak, A. Zawadzka, P. P³óciennik, K. Bartkiewicz, W. Ba³a

26 We.P.26 Automatic estimation of stacking fault density in SiC specimens imaged by transmission electron microscopy
***S.G. Stanciu**, D. Coltuc, G.A. Stanciu, A. Andreadou, A. Mantzari, E.K. Polychroniadis*

Coffee break (15:30 – 16:00)	***Coffee break*** (15:50 – 16:20)	***Coffee break*** (15:40 – 16:00)	***Coffee break*** (15:35 – 16:00)	***Coffee break*** (15:45 – 16:10)	***Coffee break*** (15:20 – 15:50)
SESSION We.D1 (16:00 – 17:55) ICTON X *Chair: **Christine Tremblay***	**SESSION We.D2** (16:20 – 18:00) SWP XI (WG2 III) *Chair: **Eugene Avrutin***	**SESSION We.D3** (16:00 – 17:55) WAOR IV *In honor of Fabio Neri* *Chair: **Halina Elbiaze***	**SESSION We.D4** (16:00 – 18:00) ESPC IV *Chair: **Ignac Bugar***	**SESSION We.D5** (16:10 – 17:40) CTS I *Chair: **Vladimir Rastorguev***	**SESSION We.D6** (15:50 – 17:40) OASE II *Chair: **Jiajia Chen***
16:00 We.D1.1 A photon counting estimates distribution of the average number of photons in coherent pulses (*Invited*) *J.C.S. Castro, **H.M. Salgado***	16:20 We.D2.1 Nonlinear interactions of optical pulses in a slow-mode nanowires (*Invited*) ***N. Dubreuil**, A. Baron, F. Kroeger, S. Trebaol, P. Delaye, R. Frey, G.P. Agrawal*	16:00 We.D3.1 Scalable optical packet switch architecture for low latency and high load computer communication networks (*Invited*) ***N. Calabretta**, S. Di Lucente, Y. Nazarathy, O. Raz, H. Dorren*	16:00 We.D4.1 Anomalous light propagation, finite size-effects and losses in real 3D photonic nanostructures (*Invited*) ***M. Botey**, G. Lozano, H. Míguez, L.A. Dorado, R.A. Depine, J. Martorell*	16:10 We.D5.1 Technologies for future automotive high speed networks (*Invited*) ***P. De Pauw**, J. Roels, R. Pérez de Aranda*	15:50 Overview and evaluation of WDM-based passive optical access technologies ***A. Autenrieth, K. Grobe***
16:20 We.D1.2 Implementation of a high speed time resolved error detector utilising a high speed FPGA (*Invited*) ***J.A. O'Dowd**, V.M. Bessler, S.K Ibrahim, A.J. Walsh, F.H. Peters, B. Corbett, B. Roycroft, P.O. Brien, A.D. Ellis*	16:40 We.D2.2 Evanescent wave coupling in hybrid III-V/SOI nanolaser (*Invited*) *A. Bazin, Y. Halioua, T. Karle, P. Monnier, G. Roelkens, I. Sagnes, R. Raj, **F. Raineri***	16:20 We.D3.2 Design of a sub-microsecond carrier class switch-router: The Omnipresent Ethernet approach (*Invited*) ***A. Gumaste***	16:20 We.D4.2 Strong light-matter interaction between guided Bloch surface waves and quantum-well excitons (*Invited*) ***M. Liscidini**, D. Gerace, D. Sanvitto, D. Bajoni*	16:30 We.D5.2 New modes of operation of the photoparametric amplifier for automotive applications (*Invited*) *H.A. Alhagagi, **R.J. Green**, M.S. Leeson, E.L. Hines*	16:10 CAPEX assessment of NGOA concepts: Cost per line ***D. Breuer***
16:40 We.D1.3 OSNR monitoring using Hi-Bi FBG for 10 Gbit/s optical networks ***A.O.P. Sousa**, C.A.F. Marques, R. Nogueira,*	17:00 We.D2.3 Stimulated Raman scattering in quantum dots and nanocomposites silicon based materials (*Invited*) ***L. Sirleto**, M.A. Ferrara, C. D'Addio, I. Rendina,*	16:40 We.D3.3 Interconnecting two intra-domain wavelength routed optical networks using an optical packet switch (*Invited*) ***H. Øverby***	16:40 We.D4.3 Laser polymerization of photonic crystals for collimation of beams at visible wavelengths (*Invited*) *L. Maigyte,*	16:50 We.D5.3 Challenges and improvements in communication with vehicles and devices moving with high-speed (*Invited*) ***K. Kastell***	16:30 Status of deployments and regulations in Asia Pacific ***S. Hanatani***